Torsional resistance tests on gutta-percha removal Ni-Ti files
(ガッタパーチャ除去用 Ni-Ti ファイルの疲労破断試験)

日本大学松戸歯学部歯内療法学講座

助手　　三浦　浩
准教授　　辻本　恭久

（指導：松島　潔　教授）

Abstract

We performed torsional resistance tests to examine the Protaper Retreatment D1, D2 and D3 and the NRT-GPR 3N and 4N, which are Ni-Ti files used to remove gutta-percha in root canal retreatment. On cyclic fatigue failure tests, the D1 was the quickest to break, and the 4N took the longest to break. Torsional bending tests showed the fracture angle to be largest for the 4N, which was significantly different from that of all the other files ($p<0.01$). There were no significant differences among the D1, D2 and D3. Torsional torque tests showed that the superelastic D1, that has the largest diameter, had the largest fracture torque. Files with larger diameters had higher fracture torques. On bending torque test, the D1 differed significantly from all the other files ($p<0.01$). Significant differences were also seen between different versions of the same file type ($p<0.01$). All of the fracture surfaces of files used in torsional resistance tests in the present experiment showed SEM findings that appear to be instantaneous breakage.

The results of this experiment indicated that torsional resistance test values varied according to differences in file properties and shape. It may be necessary to consider these results when using files in clinical practice.

Introduction

Outcomes following root canal retreatment in endodontic therapy have not been particularly favorable to date (1). There are various reasons why this is the case, one of which is that infected gutta-percha in the apical area is not being removed completely, becoming a source for further infection in the root canal and preventing healing of the periapical lesion (2). The shape of the root canal system is very complex, and the interior cannot be observed with the naked eye. Currently, it is recommended to use a microscope while executing root canal treatment. When performing root canal retreatment, it is very difficult to manipulate hand implements under a microscope to remove root canal filler, leading to long treatment times. As an alternative, many researchers have reported the use a Ni-Ti file with a rotary engine (3-8). According to these reports, the rotary Ni-Ti file can remove gutta-percha from the root canal more quickly than hand implements. There have been many reports of various torsional resistance tests performed on Ni-Ti files in use (9-15). In addition, various designs of gutta-percha removal Ni-Ti files have been documented. Lopes *et al.* (13) reported torsional resistance tests on two major files -- the ProTaper Universal retreatment file

(Maillefer/Dentsply, Ballaigues, Switzerland) and the Mtwo retreatment file (VDW, Munich, Germany). NRT-GPR gutta-percha removal file (MANI, Utsunomiya, Japan) has recently begun selling that is different from those of other companies in that it rotates faster (1000 min^{-1}), and that it is available in stainless steel for removing gutta-percha from the upper portions of the root canal, and in Ni-Ti for removing it from the periapical area or curved parts of the canal. This new file has only 1 cutting edge and one groove, while the ProTaper Universal retreatment file and Mtwo retreatment file have 3 and 2 cutting edges, respectively.

The purpose of this study was to compare the ProTaper Universal retreatment file ("Protaper Retreatment") and NRT-GPR Ni-Ti file as two differently shaped gutta-percha removal files by performing various types of torsional resistance tests, and to examine the fracture surfaces under a scanning electron microscope in order to obtain useful information for clinical practice.

Materials and Methods

The gutta-percha removal files used in the experiment were the D1, D2 and D3 Protaper Retreatment, and the MANI brand 3N and 4N NRT-GPR Ni-Ti files. The specifications for each are shown in Table 1.

1. Cyclic fatigue failure test: This test was performed according to the procedures described by Zinelis *et al.* (16). We constructed the test apparatus shown in Fig. 1 (made by MANI). Each file was rotated at 200 min^{-1} with the tip bent (anticipating a curved canal), and the time to fracture was measured. The apparatus was adjusted so that the minimum radius would be at 4 mm from the file tip. The sample size for this test was 5 of each type of file.
2. Angular deflection tests (torsional bending test): This test was performed according to ISO3630-1 (17).
    1) Torsional torque test: As shown in Fig. 2, each file was fixed in place at 3 mm from the tip. The file was twisted until it fractured, and the fracture angle and maximum torque were measured. The sample size for this test was 5 of each type of file.
    2) Bending torque test: As shown in Fig. 2, each file was fixed in place at

3 mm from the tip. The file was bent to a 45° angle and the maximum torque was measured. The sample size for this test was 5 of each type of file.

Analysis was performed with RTG-1250 with MSTAT software (A&D Co., Ltd., Tokyo, Japan).

3. Scanning electron microscope (SEM) examination of factors causing fatigue fracture

The SEM (Hitachi S-3400N, Hitachi High-technologies Corp., Tokyo, Japan) was used to observe the fatigue fracture surfaces of each file. The vacuum degree was set at 40 Pa·s, and the accelerating voltage was set at 15 kV.

4. Observation of file fracture surfaces

The fractured part at 3 mm from the tip of each file was scanned into AutoCAD LT 2002 (Autodesk. Inc., Japan). The area ratio of the severed part to the remaining part was calculated, and the cross sectional area was calculated. Area calculations were performed with the area calculation function of IM-CAD/LT Release 4.0 for AutoCAD LT 2002 drafting software.

5. Statistical analysis

Results were statistically analyzed by one-way analysis of variance (ANOVA) and Tukey's test.

Results

1. Cyclic fatigue failure test

   Time to fracture for each file is shown in Fig. 3A. The file with the shortest time to fracture was the D1, followed by the D2, 3N, D3 and 4N. The time was significantly shorter between D1 and all other types ($p<0.01$). The 4N file had the longest time to fracture, which was significantly different from that of the 3N, D1 and D2 at $p<0.01$ and from that of the D3 at $p<0.05$. Time to fracture did not differ significantly between the 3N and the D2 or D3. Within the same type of file, time to fracture differed between the 3N and the 4N for the NRT-GPR and between the D1, D2, and D3 for the Protaper Retreatment. Within the same type of file, larger D_1 diameter was associated with shorter fracture time.

2. Angular deflection tests

   1) Torsional bending test: The torsional bending fracture angles for each type of file are shown in Fig. 3B. The fracture angle was largest for the 4N file, which differed significantly from that of all the other files ($p<0.01$). The next largest fracture angle was seen in 3N, which

differed significantly from that of the 4N, D1 or D3 at $p<0.01$, and from that of the D2 at $p<0.05$. Within the same type of file, the NRT-GPR 3N differed significantly from the 4N ($p<0.01$), but no significant differences were seen between the Protaper Retreatment D1, D2 and D3.

2) Torsional torque test: The results of torsional torque tests are shown in Fig. 3C. The D1 had the largest fracture torque, while the D3 had the smallest. The D1 differed significantly from the 3N at $p<0.05$, and from the rest of the files at $p<0.01$. The D3 differed significantly from all the other files at $p<0.01$. Within the same type of file, fracture torque differed significantly between the 3N and 4N for the NRT-GPR and between the D1, D2, and D3 for the Protaper Retreatment ($p<0.01$). Values tended to increase with thicker files.

3) Bending torque test: The results of bending torque tests are shown in Fig. 3D. The D1 showed the highest values, and differed significantly from all the other files ($p<0.01$). The 4N did not differ significantly from the D3, but it did differ significantly from D2 at $p<0.05$ and from all the other types at $p<0.01$. The 3N differed significantly from all

the other types ($p<0.01$). Within the same type of file, fracture torque differed significantly between the 3N and 4N for the NRT-GPR and between the D1, D2 and D3 for the Protaper Retreatment ($p<0.01$).

3. SEM examination of factors causing fatigue fracture

Fig. 4 and 5 show SEM images of the fracture surfaces of each file. The fracture surface of every file showed dimpling with microvoids.

Fig. 6 shows the cross sections at the part 3 mm from the tip for each type of file. The area ratio was the same for the Protaper Retreatment files, at 61:39, but differed among NRT-GPR types, with 72:28 for the 3N and 76:24 for the 4N. The order of cross sectional area from largest to smallest, as shown in Table 2, was D1>3N>D2>4N>D3. This was consistent with the length ratio of the diameter for each file calculated from the taper: D1, 0.57 mm; 3N, 0.52 mm; D2, 0.49 mm; 4N, 0.42 mm; and D3, 0.41 mm.

Discussion

Root canal retreatment must always be preceded by removing the gutta-percha that was previously present in the root canal. There are various types of implements for achieving this. As manual files and other hand implements are very time-consuming, gutta-percha is now removed with rotary Ni-Ti files (3-8). However, one problem associated with rotary Ni-Ti files is that they may break during use (18-20). Fractures in rotary motion may be torsional or flexural. Sattapan *et al.* (20) found that fractures of all files broken consist of 55.7% torsional fractures and 44.3% flexural fractures. In the present experiment, we performed cyclic fatigue failure tests to measure flexural fatigue. In these tests, the D1 Protaper Retreatment was the quickest to fracture, but the time to fracture lengthened with increasing D_1 in files of the same type. The same result was seen in the NRT-GPR files. This is consistent with Lopes *et al.* (13) who suggested that files with thicker shafts are more breakable. In this experiment, we adjusted the apparatus so that the minimum radius would be at 4 mm from the file tip. The diameter at the 4 mm part was 0.66 mm for D1, 0.57 mm for D2, 0.48 mm for D3, 0.56 mm for 3N, and 0.46 mm for 4N (D1>D2>3N>D3>4N). In other words, time

to fracture shortens with increasing D_1 in files of the same type. Murata *et al.* (21) conducted root canal enlargements on extracted teeth using Ni-Ti files and found that the files broke more readily when the radius of curvature of the canal was 20° or more, and that the fracture location was within 3 mm of the tip. It is possible that the part within 3 mm of the tip in Ni-Ti files becomes stressed more easily, causing breakage. Although it was expected that there would be no significant difference between the 3N and the D2 or D3, as these two files have roughly the same diameter as the 3N, SEM observation of the cross-section at the part 3 mm from the tip of each file shows that the cross sectional area decreases from D1>3N>D2>4N>D3. There must therefore be other factors causing this difference. The cutting edge of the NRT-GPR is R-Phase Ni-Ti, which is different from the general superelastic Ni-Ti files and becomes permanently distorted to a certain degree in accordance with the curvature of the root canal. Material differences are thus one possible reason for the differences in cross section area.

In torsional bending tests, fracture angle was the largest for the NRT-GPR 4N. The reason why no significant differences were seen among the Protaper

Retreatment D1, D2 and D3 may be that these files are not R-Phase like the NRT-GPR files, but rather have the same properties as a general Ni-Ti file, and may therefore have roughly the same fracture limit, irrespective of file diameter. In contrast, the significant difference between the 3N and 4N may be due to differences in the diameter of flexible files.

Torsional torque tests revealed that larger diameter was associated with larger fracture torque within the same type of file. Among the NRT-GPR files, the larger diameter 3N required a higher torque to induce fracturing than the 4N, but had a smaller torsional fracture angle. As the 4N has a smaller diameter than the 3N, it also has a smaller fracture torque. However, the small diameter is also related to increased flexibility, which may increase the torsional fracture angle. Among Protaper Retreatment files, larger diameter was associated with significantly higher torsional fracture angle, but there were no significant differences in torsional fracture angle among the different files. This may be due to the characteristics of these files, but we intend to conduct further investigations to clarify the details.

Bending torque tests revealed that larger diameters were associated with lower bending torque. This is because thicker files require more torque to

bend them. Ullmann *et al.* (22) performed bending torque tests to compare the Protaper Shaper X, shaping files 1 and 2, and finishing files 1, 2 and 3, and found that larger diameter was associated with higher torque. In the present experiment, there were no differences between the different file types, but there were differences between files of different diameters for both Protaper Retreatment and NRT-GPR. In this test, there were no differences in data due to variations in crystal structure of the Ni-Ti files, suggesting that it differs from other tests and can be used to compare superelastic and shape memory Ni-Ti files.

Ni-Ti files may break, but it has been reported in the past that observing the fracture surface of a broken file under an SEM shows characteristic dimpling with microvoids (11-15, 19). Of particular interest was the observation of the dimpling that appeared when pressure was focused on the center of the shaft (19). The only study to date that also uses a retreatment file is that of Lopes *et al.*(13), who reported observing a ductile type fracture surface in the Protaper Retreatment file. There have been no prior reports on the NRT-GPR files. In the present study, dimpling with microvoids was observed in the fracture surfaces of both Protaper Retreatment and

NRT-GPR files, but this dimpling was not centrally limited, found all throughout the fracture surface. This suggests that, in the torsional resistance tests, the files used in this study did not break due to pressure focused on the center of the shaft, but rather broke across the shaft instantaneously.

Typically, the mechanisms of torsional failure of instruments are expected to be as described elsewhere. During the application of torque in clockwise rotation, elastic deformation initially occurs on the shaft of the instrument in an area next to the point of tip immobilization. The continuous application of torque then exceeds the yield point of the material, causing plastic deformation characterized by unwinding of the cutting spiral. This plastic deformation increases the mechanical hardening of the material, with a consequent decrease in plasticity. As the torque continues, it may overcome the breaking point of the instrument near the area of tip immobilization (9-12). However, the fracture surfaces observed in the present study were fracture surfaces of files after undergoing torsional resistance tests, and were not the area of tip immobilization after torsional fracture tests. The surfaces observed in this study were fractured from fatigue after repeated

shrinking and stretching. This may be slightly different from previous reports (11-15, 19) in that the break occurred instantaneously right across the entire fracture surface, creating a fracture from fatigue in the entire shaft. When using rotary gutta-percha removal Ni-Ti files in clinical practice, it is important to remember to use a file that is thinner than the diameter of the root canal to prevent the file from cutting into the root canal wall, and to consider the duration of file usage and number of times used. It may also be preferable to use a torque control system or other tool to control the amount of force being applied to the file.

Conclusions

We performed torsional resistance tests on the Protaper Retreatment D1, D2 and D3, as well as the NRT-GPR 3N and 4N, which are Ni-Ti files used to remove gutta-percha in root canal retreatment, and arrived at the following conclusions:

1. In torsional resistance tests, the Protaper Retreatment D1 broke the most quickly. The NRT-GPR 4N took the longest to break.
2. Torsional bending tests showed the fracture angle to be largest for the NRT-GPR 4N, which was different significantly from that of all the other files ($p<0.01$). There were no significant differences between the Protaper Retreatment D1, D2 and D3.
3. Torsional torque tests showed that the superelastic Protaper Retreatment D1, that has the largest diameter, had the largest fracture torque. Files with larger diameters had higher fracture torques.
4. In bending torque tests, larger diameter was associated with higher bending torque. The Protaper Retreatment D1 differed significantly from all the other files ($p<0.01$). Significant

differences were also seen between different versions of the same file type ($p<0.01$).

5. When examining the cause of fatigue fracture, all of the fracture surfaces of files used in torsional resistance tests in the present experiment showed characteristic SEM findings that are consistent with instantaneous breakage.

These results suggest that, while torsional resistance test values varied according to differences in file properties and shape. Therefore, when using gutta-percha removal files in clinical practice, it may be important to prevent the file from cutting into the root canal wall, to consider duration of file usage and number of times used, and to control the amount of force being applied to the file.

References

1. Friedman S, Mor C: The success of endodontic therapy--healing and functionality. J Calif Dent Assoc, 32: 493-503, 2004.
2. Noiri Y, Ehara A, Kawahara T, Takemura N, Ebisu S: Participation of bacterial biofilms in refractory and chronic periapical periodontitis. J Endod, 28: 679-83, 2002.
3. Schirrmeister JF, Wrbas KT, Schneider FH, Altenburger MJ, Hellwig E: Effectiveness of a hand file and three nickel-titanium rotary instruments for removing gutta-percha in curved root canals during retreatment. Oral Surg Oral Med Oral Pathol Oral Radiol Endod, 101: 542-7, 2006.
4. Kosti E, Lambrianidis T, Economides N, Neofitou C: Ex vivo study of the efficacy of H-files and rotary Ni-Ti instruments to remove gutta-percha and four types of sealer. Int Endod J, 39: 48-54, 2006.
5. Gergi R, Sabbagh C: Effectiveness of two nickel-titanium rotary instruments and a hand file for removing gutta-percha in severely curved root canals during retreatment: an ex vivo study. Int Endod J, 40: 532-7, 2007.
6. Giuliani V, Cocchetti R, Pagavino G: Efficacy of ProTaper universal

retreatment files in removing filling materials during root canal retreatment. J Endod, 34: 1381-4, 2008.

7. Yilmaz Z, Karapinar SP, Ozcelik B: Efficacy of rotary Ni-Ti retreatment systems in root canals filled with a new warm vertical compaction technique. Dent Mater J, 30: 948-53, 2011.
8. Mollo A, Botti G, Prinicipi Goldoni N, Randellini E, Paragliola R, Chazine M, Ounsi HF, Grandini S: Efficacy of two Ni-Ti systems and hand files for removing gutta-percha from root canals. Int Endod J, 45: 1-6, 2012.
9. Seto BG, Nicholls JI, Harrington GW: Torsional properties of twisted and machined endodontic files. J Endod, 16: 355-60, 1990.
10. Rowan MB, Nicholls JI, Steiner J: Torsional properties of stainless steel and nickel-titanium endodontic files. J Endod, 22: 341-5, 1996.
11. Park SY, Cheung GS, Yum J, Hur B, Park JK, Kim HC: Dynamic torsional resistance of nickel-titanium rotary instruments. J Endod, 36: 1200-4, 2010.
12. Yum J, Cheung GS, Park JK, Hur B, Kim HC: Torsional strength and toughness of nickel-titanium rotary files. J Endod, 37: 382-6, 2011.
13. Lopes HP, Elias CN, Vedovello GA, Bueno CE, Mangelli M, Siqueira JF

Jr.: Torsional resistance of retreatment instruments. J Endod, 37: 1442-5, 2011.

14. Kim JY, Cheung GS, Park SH, Ko DC, Kim JW, Kim HC: Effect from cyclic fatigue of nickel-titanium rotary files on torsional resistance. J Endod, 38: 527-30, 2012.
15. Kim HC, Kwak SW, Cheung GS, Ko DH, Chung SM, Lee W: Cyclic fatigue and torsional resistance of two new nickel-titanium instruments used in reciprocation motion: Reciproc versus WaveOne. J Endod, 38: 541-4, 2012.
16. Zinelis S, Darabara M, Takase T, Ogane K, Papadimitriou GD: The effect of thermal treatment on the resistance of nickel-titanium rotary files in cyclic fatigue. Oral Surg Oral Med Oral Pathol Oral Radiol Endod, 103: 843-7, 2007.
17. International Organization for Standardization. ISO 3630-1 : Dentistry –Root-canal instruments－part 1: General requirements and test methods, Geneva, Switzerland, 2008.
18. Tsujimoto Y, Miura H, Yamazaki M: Observation of breakage and extension of ProFile Series 29 and Orifice Shapers endodontic files after

clinical use. Dent Jpn, 39: 52-6, 2003.

19. Parashos P, Messer HH: Rotary NiTi instrument fracture and its consequences. J Endod, 32: 1031-43, 2006.

20. Sattapan B, Nervo GJ, Palamara JE, Messer HH: Defects in rotary nickel-titanium files after clinical use. J Endod, 26:161-5, 2000.

21. Murata T, Kawamoto K, Kozuka M, Tsujimoto Y, Yamazaki M: Evaluation of enlargement of root canal and changes of shape using GT Rotary files at different rpm. Japan J Coserv Dent, 44:900-904, 2001.

22. Ullmann CJ, Peters OA: Effect of cyclic fatigue on static fracture loads in ProTaper nickel-titanium rotary instruments. J Endod, 31: 183-6, 2005.

Table 1. States of files

	NRT-GPR		Protaper Retreatment		
	3N	4N	D1	D2	D3
Materials	Ni-Ti	Ni-Ti	Ni-Ti	Ni-Ti	Ni-Ti
Size(D_1)	#40	#30	#30	#25	#20
File taper	4%	4%	9%	8%	7%
File length	21mm	21mm	16mm	18mm	22mm
Number of cutting edge	1	1	3	3	3

Table 2. Cross section area of each gutta-percha removal file

Product name	Model No.	①	②	③
NRT-GPR	3N	0.212	0.153	0.059
	4N	0.139	0.105	0.033
Protaper Retreatment	D1	0.255	0.156	0.100
	D2	0.189	0.115	0.074
	D3	0.132	0.081	0.051

①Cross-section area of D_3 (mm^2) ②Cross-section area of the cutting portion (mm^2) Remained cross-section area (mm^2)

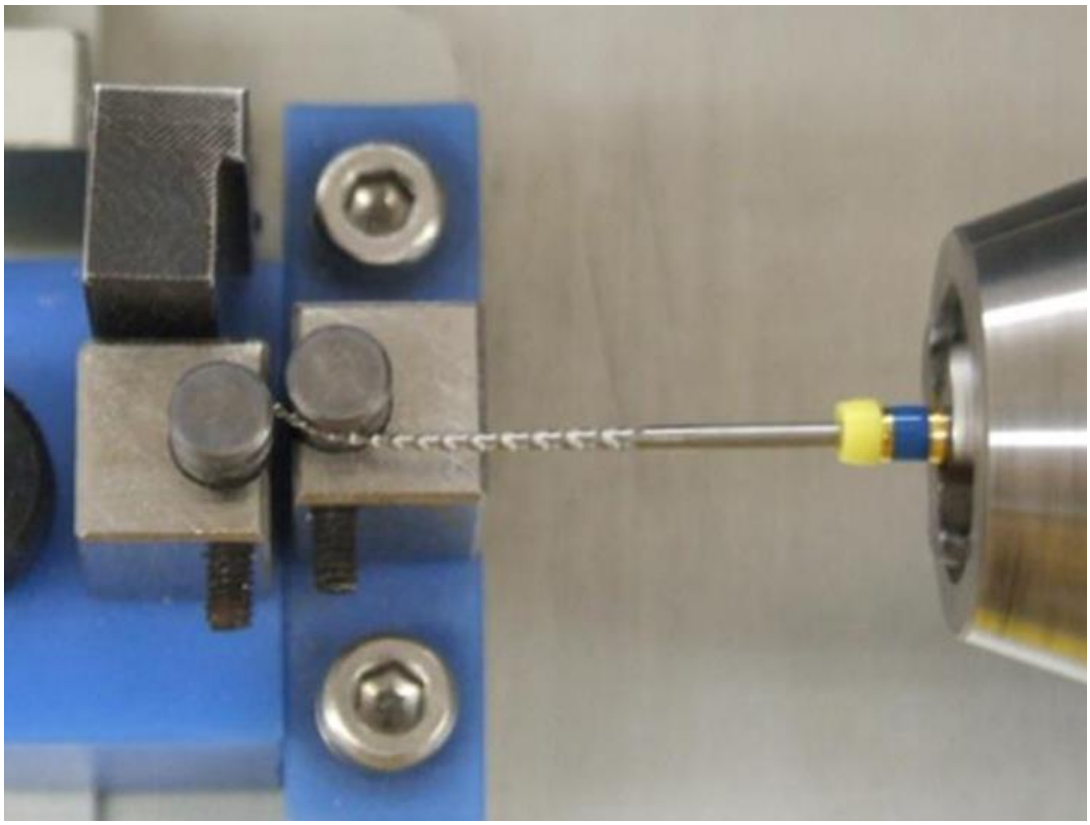

Fig. 1 Test device: MANI original cyclic fatigue test machine.

Rotation speed is 200min^{-1}.

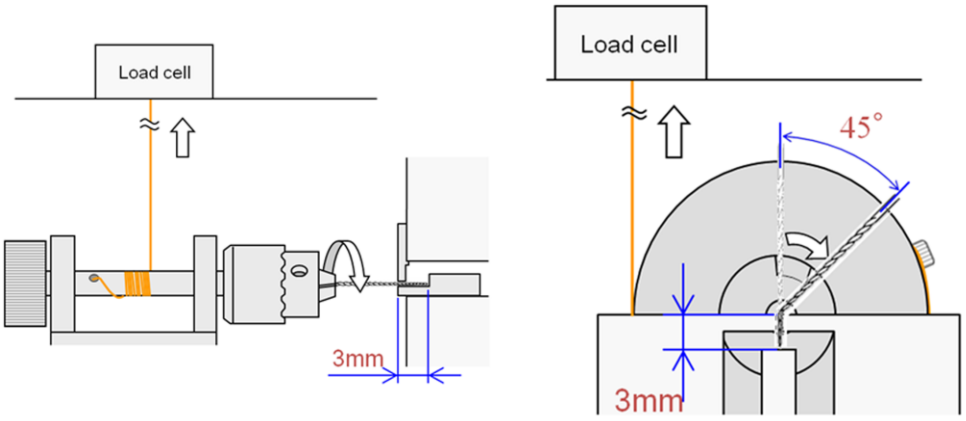

Fig. 2 Torsion torque test and Bending torque test.

(Left) Torsion torque test: Tighten the sample at 3mm from the tip with the chuck. Measure the angular deflection and maximum torque at fracture.

(Right) Bending torque test: Tighten the sample at 3mm from the tip with the chuck. Measure the maximum torque required to bent the sample to 45°.

A

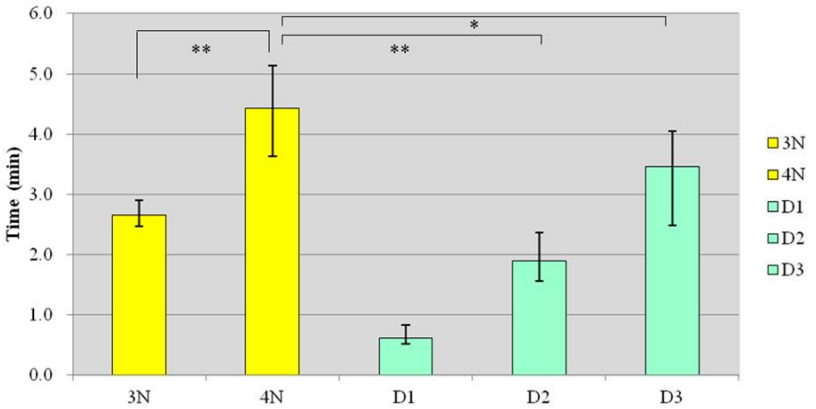

D1 vs all groups $p < 0.01$

** : $p < 0.01$

* : $p < 0.05$ (n=5)

B

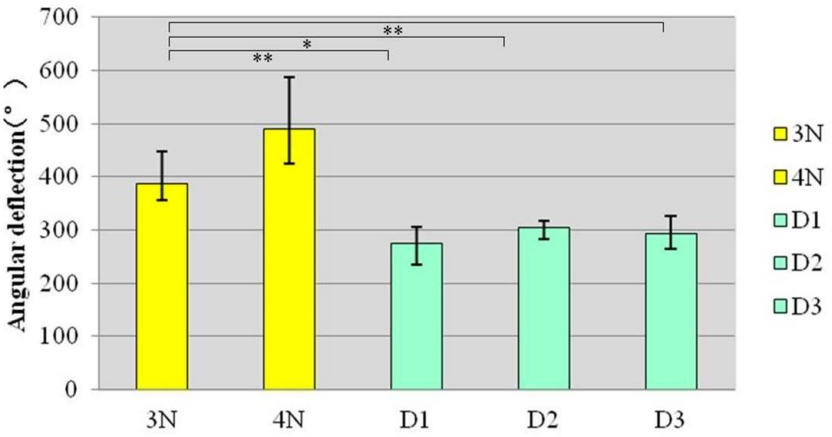

4N vs all groups $p < 0.01$

** : $p < 0.01$

* : $p < 0.05$ (n=5)

C

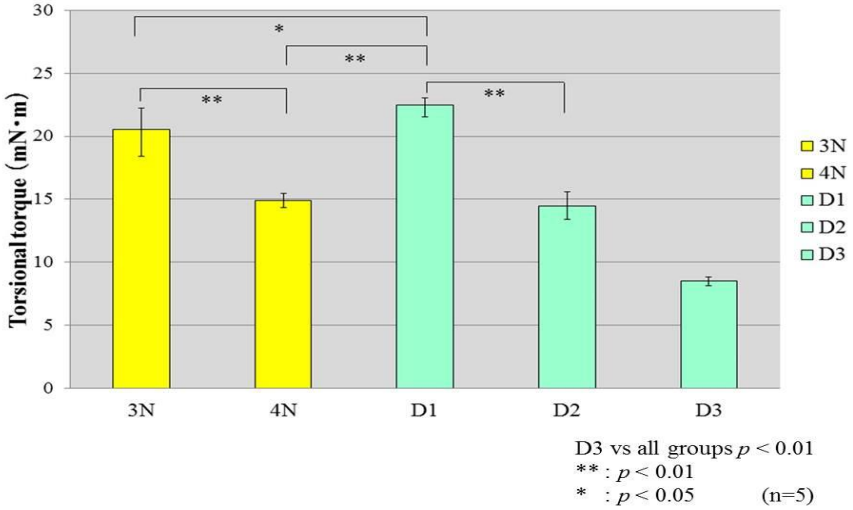

D

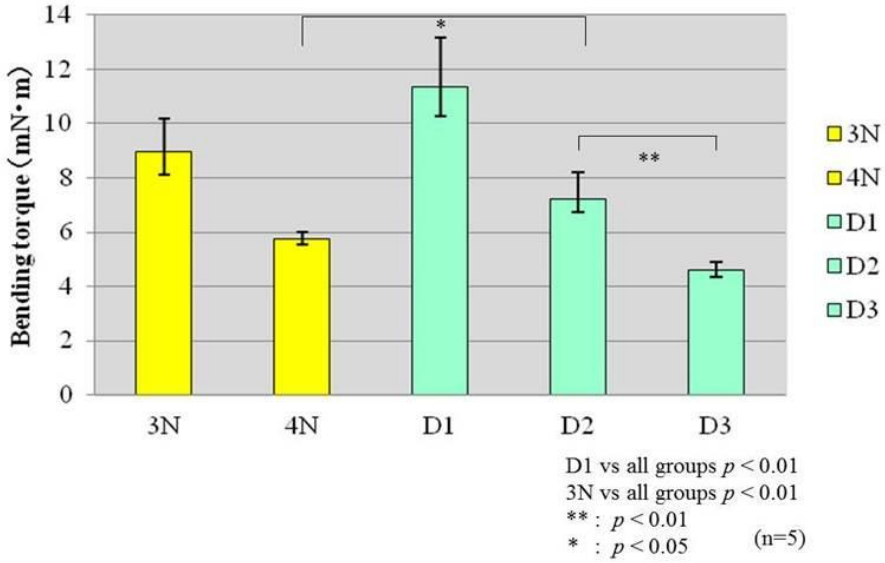

Fig. 3 Torsional resistance test results

A: Cyclic fatigue failure test　　B: Torsional bending test

C: Torsional torque test　　D: Bending torque test

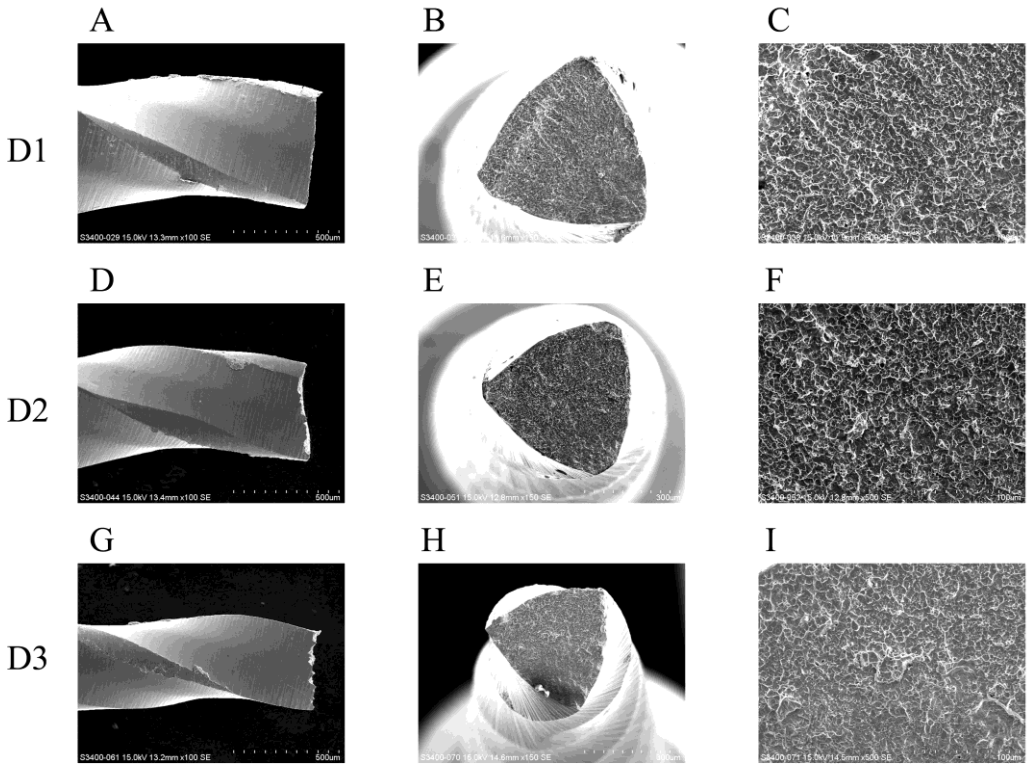

Fig. 4 Protaper Retreatment instrument (after time to fracture)

Plastic deformation observed on the helical shaft, D1(A), D2(D), D3(G). (original magnification, 100x)

Fractured surface shows the dimpling and microvoid, D1(B), D2(E), D3(H). (original magnification, 150x) Higher magnification (original magnification, 500x) of the fractured surface, D1(C), D2(F), D3(I).

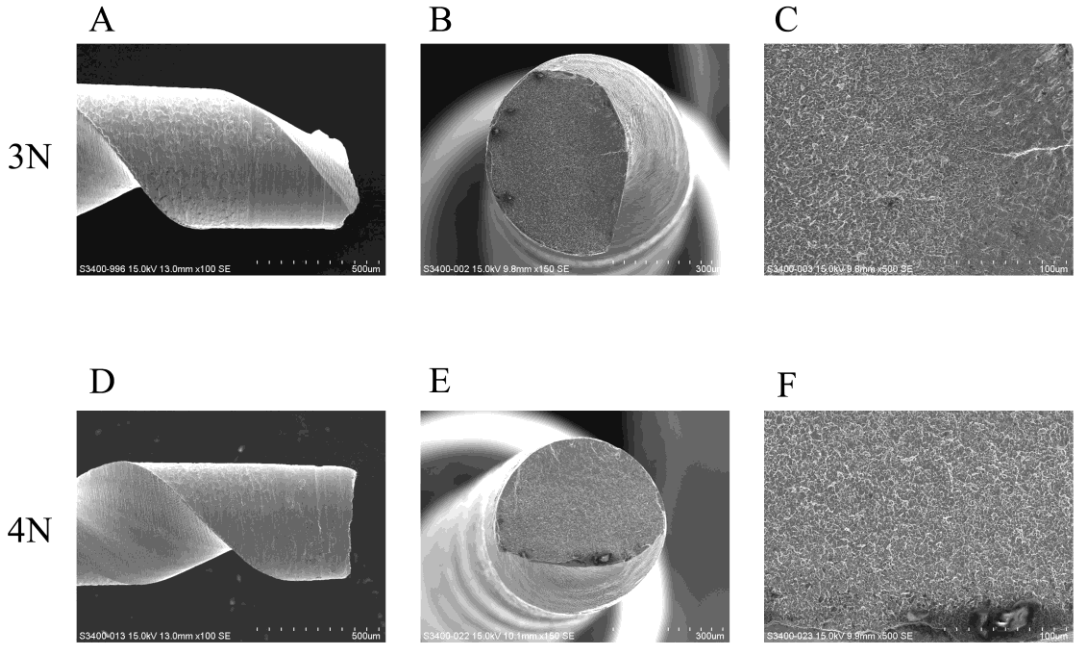

Fig. 5 NRT-GPR instrument (after time to fracture)

Plastic deformation observed on the helical shaft, 3N(A), 4N(D). (original magnification, 100x)

Fractured surface shows the dimpling and microvoid, 3N(B), 4N(E). (original magnification, 150x)

Higher magnification (original magnification, 500x) of the fractured surface, 3N(C), 4N(F).

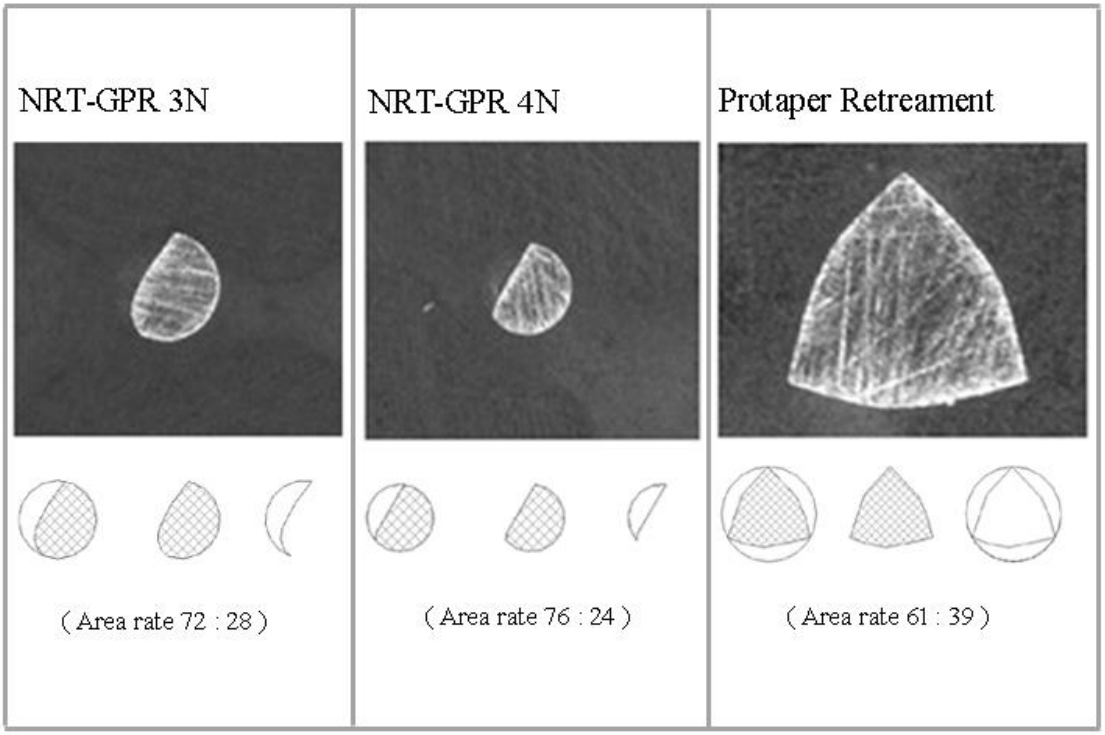

Fig. 6 Cross-section of NRT-GPR and Protaper Retreatment instrument at D3

(left): NRT-GPR 3N (original magnification, 100x), (center): NRT-GPR 4N (original magnification, 100x), (right): Protaper Retreatment D1(original magnification, 150x).

Area rate was calculated and showed.